Effects of Rolling Reduction on Critical Current Density and Microstructure of Bi-2212 Wires

Jianyi Jiang, *Senior Member, IEEE*, Jozef Kvitkovic, Caitlynn Linville, Jamia Brown, Jakeyvan Jones, Daniel S. Davis, *Member, IEEE*, Youngjae Kim, *Member, IEEE*, Fumitake Kametani, *Member, IEEE*, Ulf P. Trociewitz, *Senior Member, IEEE*, Eric E. Hellstrom, *Senior Member, IEEE*, David C. Larbalestier, *Life Fellow, IEEE*, Jean-Francois Croteau, Christopher Escobar, and Tengming Shen

***Abstract*—Bi-2212 Rutherford cables have been fabricated into flat racetrack coils and canted-cosine-theta dipole magnets. The performance gap between the magnets made with Rutherford cables and the "short-sample-limit" is about 30%. To better understand the influence of Rutherford cable processing on the strand performance, we studied three Bi-2212 wires with filament architectures of 37 × 18 and 55 × 18 and diameters of 0.8 and 1.0 mm. To simulate the deformation caused by cabling process, the three wires were rolled with thickness reductions ranging from 10% to 30%. The aspect ratios of rolled strands are between 1.29 and 2.05. The low aspect-ratio wire is also an interesting form for fabricating solenoid coils with higher packing density. The round and rolled strands were heat-treated under 50 bar and with maximum heat treatment temperatures of 885.5 °C and 890.5 °C. The rolling deformation reduced filament size uniformity, resulting in filament merging in fully heat-treated wires. It was found that rolling reduction reduced wire critical current density (J_E) by 16 to 18%, but the J_E decrease saturated at 15 to 20% of the thickness reduction. It is believed that the reduced J_E results from the filament merging caused by rolling and non-uniform shrinking during overpressure heat treatment.**

***Index Terms*—Bi-2212 wire, critical current density, superconductor, superconducting magnet.**

Received 26 September 2024; revised 6 December 2024; accepted 11 December 2024. Date of publication 16 December 2024; date of current version 26 December 2024. This work is supported by US DOE Accelerator R&D and Production (ARDAP). This work at National High Magnetic Field Laboratory was also supported in part by US DOE OHEP under Grant DE-SC0010421 and Grant DE-SC0024610, in part by NSF under Award DMR-2128556, and in part by the State of Florida. Work at Lawrence Berkeley National Laboratory was supported in part by the US DOE, Office of Science under Contract Number DE-AC02-05CH11231. *(Corresponding author: Jianyi Jiang.)*

Jianyi Jiang is with Applied Superconductivity Center, National High Magnetic Laboratory, Florida State University, Tallahassee, FL 32310 USA (e-mail: jjiang@asc.magnet.fsu.edu).

Jozef Kvitkovic, Caitlynn Linville, Jamia Brown, Jakeyvan Jones, Daniel S. Davis, Youngjae Kim, and Ulf P. Trociewitz are with Applied Superconductivity Center, National High Magnetic Field Laboratory, Florida State University, Tallahassee, FL 32310 USA.

Fumitake Kametani, Eric E. Hellstrom, and David C. Larbalestier are with Applied Superconductivity Center, National High Magnetic Field Laboratory, Florida State University, Tallahassee, FL 32310 USA, and also with the Department of Mechanical Engineering, FAMU-FSU College of Engineering, Tallahassee, FL 32310 USA.

Jean-Francois Croteau and Tengming Shen are with Lawrence Berkeley National Laboratory, Berkeley, CA 94720 USA.

Christopher Escobar is with Lawrence Berkeley National Laboratory, Berkeley, CA 94720 USA, and also with the University of California, Berkeley, CA 94720 USA.

Color versions of one or more figures in this article are available at https://doi.org/10.1109/TASC.2024.3519083.

Digital Object Identifier 10.1109/TASC.2024.3519083

I. Introduction

Bi-2212 wire is a promising high-field superconductor for applications such as high energy particle accelerators, fusion reactors, and nuclear magnetic resonance (NMR) spectrometers [1], [2], [3], [4], [5]. It is multifilamentary, available in a wide range of fine filaments and twisted filament architectures and can be made into Rutherford and other cables [6], [7], [8], [9], [10], [11], [12]. Bi-2212 Rutherford cables were fabricated into a flat racetrack coil, which achieved a wire critical current density (J_E) of 1020 A/mm^2 (4.2 K, 3.5 T) [6], and a canted-cosine-theta dipole magnet was made in 2022, generating a dipole field of 1.64 T with a 30.8 mm bore [7].

The strands of Rutherford cable are twisted, rolled, and deformed during the cabling process. We need to understand the impact of the cabling process on the performance of the Bi-2212 wire. Previous work on extracted strands from Rutherford cables showed no critical current (I_C) difference between the kinked and the straight sections [5]. The cables in [5] are 17-strand Rutherford cables (0.8 mm strands and nominal dimensions 1.4 mm × 7.8 mm) with a packing factor of 81% and a rolling reduction of 12.5% in the straight sections; the rolling reduction in the kink section may be as high as ∼20%. However, the performance gap between the magnets made with Rutherford cables and the "short-sample-limit" is about 30% [2], [7]. The deformation rate of the strands in Rutherford cable depends on the cable packing density and the strand location. Barzi et al. [13] measured the deformation of a 25-strand cable reacted at 1 bar total pressure and found that the deformation of Bi-2212 strands ranged between 5% to 30%. Traverso et al. [14] studied the effect of flattening Bi-2212 wire on the wire performance and found that the critical current increased with the wire thickness reduction of up to 20%. Since their wire heat treatments were performed in 1 bar flowing oxygen and porosity plays a critical role in limiting the critical current density in the wires reacted in 1 bar pressure [15] [16] [17], we believe that the increased critical current values in the flattened wires result from the reduced porosity.

To simulate the deformation caused by the cabling process, we rolled three Bi-2212 wires with thickness reductions ranging from 10% to 30%. The aspect ratios of rolled strands are between 1.29 and 2.05. The low aspect-ratio wire is also an interesting form for fabricating solenoid coils with higher packing density.

TABLE I
SPECIFICATIONS OF THE BI-2212 WIRES USED IN THIS STUDY

Wire ID	Filament configuration	Wire dimeter (mm)	Filling factor after densification	Average equivalent filament diameter in the round wire after densification[a] (μm)
PMM170725	55x18	0.8	0.211	10.8
PMM211105	55x18	1.0	0.199	13.6
PMM220802	37x18	0.8	0.196	13.2

[a]Average equivalent filament diameter was calculated by measuring the filament area and calculating the diameter of a circle whose area equals the measured area.

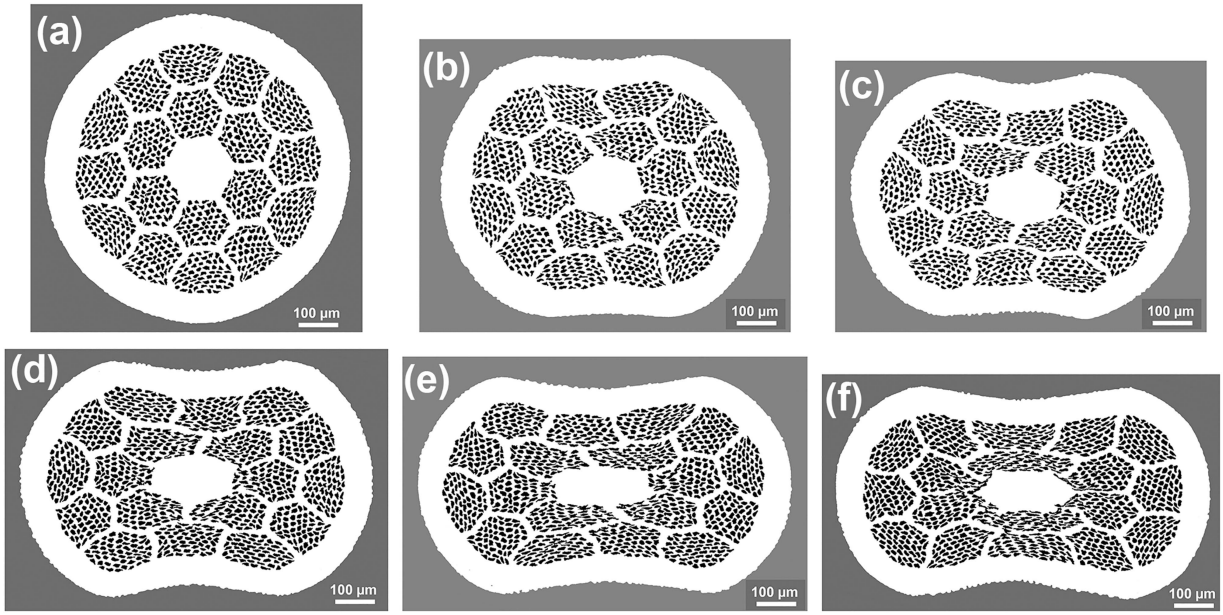

Fig. 1. Cross section images of (a) round wire, and rolled wire samples of PMM170715 (55 × 18, 0.8 mm) with thickness reduction of (b) 10%, (c) 15%, (d) 20%, (e) 25% and (f) 30% after 50 bar pre-densification heat treatment, 830 °C/12 hrs.

Here we report on the critical current density and microstructure of the aspected Bi-2212 wires after 50 bar overpressure heat treatments (OPHT).

II. EXPERIMENTAL

As listed in Table I, three Bi-2212 wires were used for this study. The three Bi-2212 wires were fabricated by Bruker OST with filament architectures of 37 × 18 and 55 × 18 and diameters of 0.8 and 1.0 mm [18], [19]. Two-meter-long pieces of the wires were rolled with thickness reduction of 10%, 15%, 20%, 25%, and 30%. 9 cm long samples that had both ends hermetically sealed were prepared for OPHT.

To analyze filament size, wire cross section area, and filament fill factor (defined as the ratio of filament cross section area to total wire cross section area), we densified the wire samples using an overpressure pre-densification heat treatment at 830 °C for 12 hours [20]. All OPHTs were done at 50 bar total pressure with an oxygen partial pressure pO_2 of 1 bar (1 bar O_2 + 49 bar Ar). The full OPHT schedule with a wide range of maximum temperatures (T_{max}) was reported previously [18]. For this study, T_{max} of 885.5 °C corresponding to peak J_E and 890.5 °C corresponding to the plateau J_E were chosen for the full OPHTs.

Critical currents of fully heat-treated wires were measured using the four-probe transport method with a 1 μV/cm criterion at 4.2 K in a magnetic field of 5 T applied perpendicular to the wire axis. Microstructures were examined with a Zeiss EVO 10 scanning electron microscope (SEM).

III. RESULTS

Fig. 1 shows optical images of transverse cross-sections of wire samples of PMM170725 (55 × 18, 0.8 mm) with different rolling deformation from 0 to 30% after the pre-densification heat treatment. The middle section of the rolled wire samples shrank more than their edge sections, forming a peanut shape after densification. The strength of the Ag-Mg alloy sheath increases and the strength of the pure Ag matrix decreases during the pre-densification process. The middle sections of the wires were deformed more by the flat rolling than the wire edges, so that the thickness of the Ag-Mg alloy sheath in the middle sections of the rolled wires was thinner than the wire edges. The thicker Ag-Mg sheath at the wire edges is stronger than that at the middle sections of the wires, resulting in more deformation in the middle section than the wire edges during the densification process.

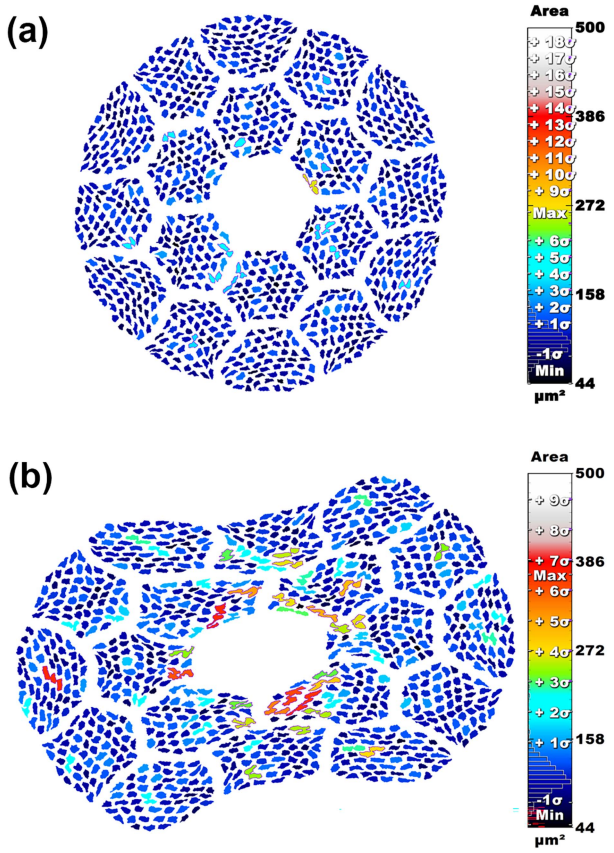

Fig. 2. Filament area distributions on transverse cross-sections after pre-densification heat treatment. Color-coded area maps from two samples, (a) round wire PMM170725 and (b) rolled PMM170725 with 20% thickness reduction. Large and merged filaments that have a large standard deviation in filament size are outlined in light colors.

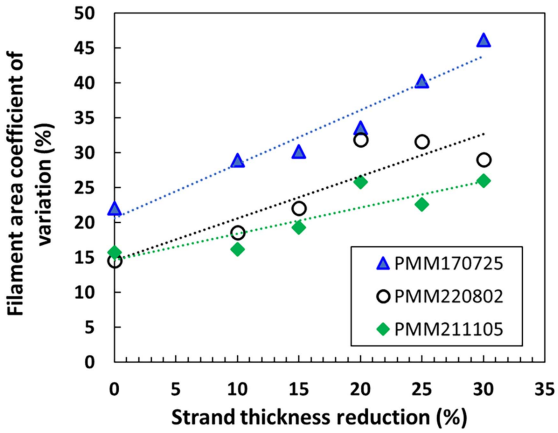

Fig. 3. Filament area coefficient of variation (CV) as a function of strand thickness reduction for wires, PMM170725 (55 × 18, 0.8mm), PMM220802 (37 × 18, 0.8 mm) and PMM211105 (55 × 18, 1.0 mm). The dashed trend lines are to guide the eye.

We define the wire aspect ratio (AR) as the maximum width divided by minimum thickness. The AR values for the aspected wires shown in Fig. 1 are 1.29, 1.48, 1.66, 1.94 and 2.05 for rolling deformation of 10%, 15%, 20%, 25% and 30%, respectively. Wire filling factors and average filament size were measured on the cross-sections of the densified wire samples

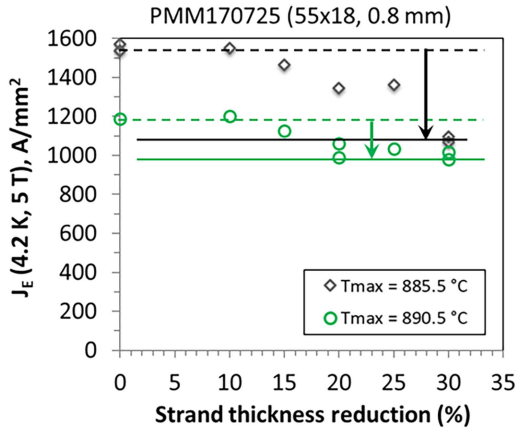

Fig. 4. J_E(4.2 K, 5 T) as a function of strand thickness reduction for wire PMM170725. The arrows from the dashed lines to the solid lines show the J_E reduction with the strand deformation. For T_{max} = 885.5 °C, J_E(4.2 K, 5 T) was reduced by 32%, while it reduced 18% for T_{max} = 890.5 °C.

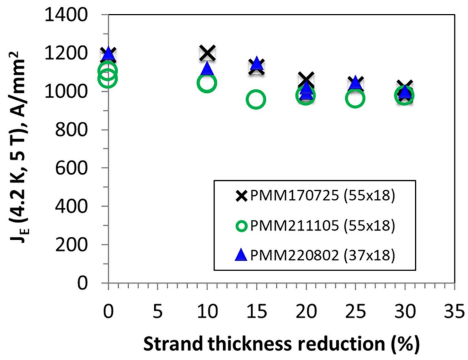

Fig. 5. J_E(4.2 K, 5 T) as a function of strand thickness reduction for three wires after 50 bar OPHT with a T_{max} of 890.5 °C. The J_E reduction of the rolled wires is less than 18%.

including rolled wires PMM211105 (55 × 18, 1.0 mm) and PMM220802 (37 × 18, 0.8 mm). As shown in Table I, the three wires have similar fill factors, about 20%, but their average filament sizes are different, in the range of 10.8 to 13.6 μm. The cross-section area values of the densified wire samples were used for the calculation of wire J_E.

Fig. 2 shows filament area distributions on transverse cross-sections of pre-densified round and aspected wires. The coefficient of variation (CV), also known as relative standard deviation, is defined as the ratio of the standard deviation (σ) to the mean (μ), CV = σ/μ,. The filament area CV value for wire PMM170725 (55 × 18, 0.8 mm) is 21.2% for the round wire, and 33.7% for the rolled wire with 20% deformation. The increased value of filament area CV in the rolled wire shows that rolling deformation reduced filament uniformity and many filaments in the central region of the rolled wires merged during rolling.

Fig. 3 compares the filament area CV as a function of wire deformation for the three wires. The smaller slopes of the trend lines shown in Fig. 3 for wires PMM220802 and PMM211105 indicate that the filament uniformity of the wires with larger filament size is less sensitive to the rolling deformation.

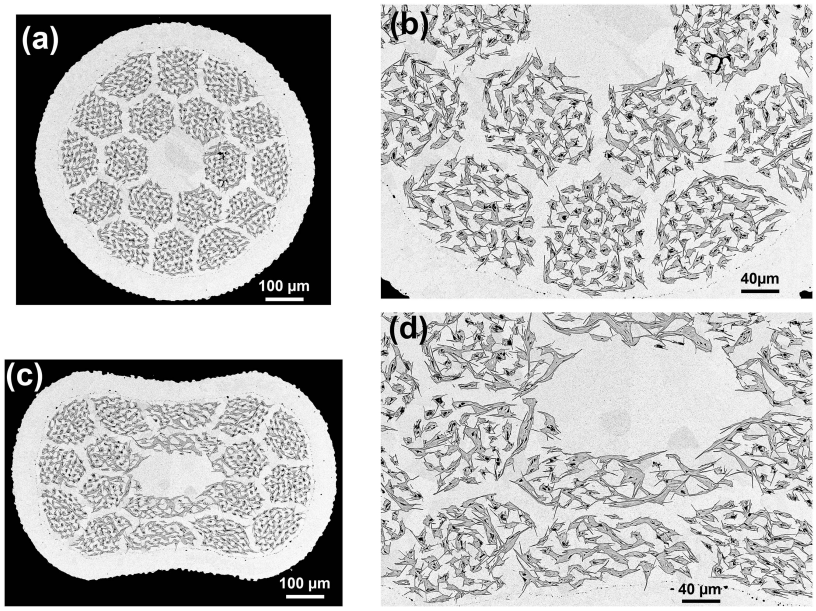

Fig. 6. SEM images of cross-sections of (a) and (b) round wire, (c) and (d) rolled wire with 20% deformation for wire PMM170725 (55 × 18, 0.8 mm) after 50 bar OPHT with $T_{\max} = 885.5$ °C.

Fig. 4 shows J_E(4.2 K, 5 T) of round and rolled samples of wire PMM170725 after 50 bar OPHTs with $T_{\max}$ of 885.5 °C and 890.5 °C. For $T_{\max} = 885.5$ °C, J_E(4.2 K, 5 T) was reduced by 32%. For $T_{\max} = 890.5$ °C, a temperature normally used for coil heat-treatment, J_E(4.2 K, 5 T) reduction was 18% and it saturated at 20% strand deformation.

Fig. 5 plots J_E as a function of strand deformation for the three wires. J_E(4.2 K, 5 T) reduction was 16% and 17% for wire PMM211105 and PMM220802, respectively.

As shown in Fig. 6, the round wire shrank uniformly with a diameter reduction of about 3% after the full OPHT at 50 bar while the middle sections of the rolled wire samples shrank more than their edge sections, forming a peanut shape which was also observed in the pre-densified samples (shown in Fig. 1). Comparing Fig. 6(d) with Fig. 6(b), it can be seen that the rolled wire formed more merged filaments, a phenomenon related to increased filament sausaging and reduced J_E value [18], [19], [21], [22].

IV. Discussion

As shown in Figs. 2 and 3, rolling deformation reduced filament uniformity and promoted filament merging after 50 bar OPHT. As listed in Table I, 1.0 mm PMM211105 (55 × 18) and 0.8 mm PMM220802 (37 × 18) have larger average filament sizes (13.6 and 13.2 μm, respectively) than 0.8 mm PMM170725, whose filament size is 10.8 μm. Since all three wires have similar fill factors (about 20%), the wire with a larger filament size also has a larger separation between filaments. The smaller slopes of the trend lines shown in Fig. 3 for wires PMM220802 and PMM211105 indicate that the filament uniformity and merging of filaments during the rolling of the wires with larger filament size are less sensitive to the rolling deformation.

As we reported previously [18], wires heat-treated at the low end of $T_{\max}$ (885.5 °C) showed the highest J_E, more uniform filaments and fewer merged filaments. Fig. 4 shows that the samples heat treated at 885.5 °C had a larger degradation with increased rolling deformation compared with the samples heat treated at 890.5 °C. This result indicates that filament nonuniformity caused by rolling reduction played a major role in reduced J_E in the samples heat treated with lower $T_{\max}$ (855.5 °C).

As shown in Figs. 4 and 5, all the aspected wires except the wires with 10% deformation showed lower J_E. Wires with 10% deformation had almost the same J_E as the round ones. Marken et al. [3] studied aspected wires with aspect ratio up to 2.0 in 2006 and their wire samples were heat-treated in 1 bar total pressure. The 1 bar heat-treated wire samples did not show a decrease in J_E with increasing aspect ratio. This indicates that in these 1 bar samples the porosity played a major role in limiting the critical current density rather than the change of the filament uniformity by deformation.

V. Conclusion

We studied the effects of rolling deformation on the critical current density and microstructure of three Bi-2212 wires. The middle sections of the aspected wires shrank more than their edge sections after OPHT, forming a peanut shape. Rolling deformation reduced filament size uniformity, resulting in more filament merging in OPHTed wires and lower J_E. Filament size uniformity of 1.0 mm wire PMM211105 (55 × 18) and 0.8 mm wire PMM220802 (37 × 18) is less sensitive to rolling reduction than 0.8 mm wire PMM170725 (55 × 18) because of larger filament size and larger separation between filaments in wires PMM211105 and PMM220802. J_E(4.2 K, 5 T) values of the rolled wires were reduced by 16 to 18% for $T_{\max} = 890.5$ °C, but the J_E decrease saturated at 15 to 20% of the wire thickness

reduction. This J_E saturation is consistent with the earlier finding that there is no appreciable difference in J_E between the straight section and the kink section in [5].

The observed performance gap between coils made from Bi-2212 Rutherford cable and the "short-sample-limit" can be partly explained by the combined role of rolling and overpressure processing heat treatment identified in this study [7]. Recent Bi-2212 Rutherford cables are fabricated with a packing factor of 78–82%. This study indicates that it is possible to further increase the packing density to improve the overall current density of a Rutherford able coil since J_E reduction saturates at 15 to 20% of the wire thickness reduction. The observed performance gap between coils made from Bi-2212 Rutherford cable and the "short-sample-limit" can be explained by rolling deformation and additional factors, such as ceramic leakage.

ACKNOWLEDGMENT

The authors are grateful for discussions with S. Barua, A. Abuzar, A. Xu, C. Tarantini, P. J. Lee, and L. D. Cooley of the National High Magnetic Field Laboratory, D. E. Bugaris and C. Goggin of Engi-Mat, and Y. Huang and M. Brown of Bruker OST, and technical help from V. S. Griffin and W. L. Starch of the National High Magnetic Field Laboratory. The authors would like to thank Andy Lin of Lawrence Berkeley National Laboratory for his assistance with wire rolling.

The authors would like to thank Engi-Mat for providing wires PMM170725 and PMM220802 for this study.

REFERENCES

[1] D. C. Larbalestier et al., "Isotropic round-wire multifilament cuprate superconductor for generation of magnetic fields above 30 T," *Nat. Mater.*, vol. 13, no. 4, pp. 375–381, Apr. 2014, doi: 10.1038/nmat3887.

[2] T. Shen and L. Garcia Fajardo, "Superconducting accelerator magnets based on high-temperature superconducting Bi-2212 round wires," *Instruments*, vol. 4, no. 2, Jun. 2020, Art. no. 17, doi: 10.3390/instruments4020017.

[3] K. R. Marken, H. Miao, M. Meinesz, B. Czabaj, and S. Hong, "Progress in Bi-2212 wires for high magnetic field applications," *IEEE Trans. Appl. Supercond.*, vol. 16, no. 2, pp. 992–995, Jun. 2006, doi: 10.1109/tasc.2006.873262.

[4] J. Jiang et al., "High-performance Bi-2212 round wires made with recent powders," *IEEE Trans. Appl. Supercond.*, vol. 29, no. 5, Aug. 2019, Art. no. 6400405, doi: 10.1109/tasc.2019.2895197.

[5] K. Zhang et al., "Tripled critical current in racetrack coils made of Bi-2212 Rutherford cables with overpressure processing and leakage control," *Supercond. Sci. Technol.*, vol. 31, no. 10, Oct. 2018, Art. no. 105009, doi: 10.1088/1361-6668/aada2f.

[6] T. Shen et al., "Stable, predictable and training-free operation of superconducting Bi-2212 Rutherford cable racetrack coils at the wire current density of 1000 A/mm2," *Sci. Rep.*, vol. 9, no. 1, Jul. 2019, Art. no. 10170, doi: 10.1038/s41598-019-46629-3.

[7] T. Shen et al., "Design, fabrication, and characterization of a high-field high-temperature superconducting Bi-2212 accelerator dipole magnet," *Phys. Rev. Accelerators Beams*, vol. 25, no. 12, Dec. 2022, Art. no. 122401, doi: 10.1103/PhysRevAccelBeams.25.122401.

[8] L. Garcia Fajardo et al., "First demonstration of high current canted-cosine-theta coils with Bi-2212 Rutherford cables," *Supercond. Sci. Technol.*, vol. 34, no. 2, Feb. 2021, Art. no. 024001, doi: 10.1088/1361-6668/abc73d.

[9] Z.-C. Zhang, D.-S. Yang, H.-S. Zhou, J.-G. Qin, and G.-N. Luo, "Degradation mechanism of the superconducting performance of a Bi2212 cable under magnetic fields," *Supercond. Sci. Technol.*, vol. 35, no. 3, Mar. 2022, Art. no. 035004, doi: 10.1088/1361-6668/ac4ad2.

[10] D. Yang et al., "Performance of first Bi-2212 cable with pre-over pressure and over pressure heat treatment," *Supercond. Sci. Technol.*, vol. 35, no. 1, Jan. 2022, Art. no. 015007, doi: 10.1088/1361-6668/ac30ea.

[11] J.-G. Qin et al., "Manufacture and test of Bi-2212 cable-in-conduit conductor," *IEEE Trans. Appl. Supercond.*, vol. 27, no. 4, Jun. 2017, Art. no. 4801205, doi: 10.1109/TASC.2017.2652306.

[12] H. Zhao et al., "Manufacture process and cabling optimization of Bi2212 CICC," *Phys. C Supercond. Appl.*, vol. 625, Oct. 2024, Art. no. 1354579, doi: 10.1016/j.physc.2024.1354579.

[13] E. Barzi, V. Lombardo, A. Tollestrup, and D. Turrioni, "Study of effects of transverse deformation in BSCCO-2212 wires," *IEEE Trans. Appl. Supercond.*, vol. 21, no. 3, pp. 2808–2811, Jun. 2011, doi: 10.1109/TASC.2011.2106105.

[14] A. Traverso et al., "Analysis of the flattening on Bi-2212 wires due to the cabling process and its effect on their performances," *IEEE Trans. Appl. Supercond.*, vol. 34, no. 3, May 2024, Art. no. 6400605, doi: 10.1109/TASC.2023.3345290.

[15] J. Jiang et al., "Doubled critical current density in Bi-2212 round wires by reduction of the residual bubble density," *Supercond. Sci. Technol.*, vol. 24, no. 8, Aug. 2011, Art. no. 082001, doi: 10.1088/0953-2048/24/8/082001.

[16] F. Kametani et al., "Bubble formation within filaments of melt-processed Bi2212 wires and its strongly negative effect on the critical current density," *Supercond. Sci. Technol.*, vol. 24, no. 7, Jul. 2011, Art. no. 075009, doi: 10.1088/0953-2048/24/7/075009.

[17] J. Jiang et al., "Reduction of gas bubbles and improved critical current density in Bi-2212 round wire by swaging," *IEEE Trans. Appl. Supercond.*, vol. 23, no. 3, Jun. 2013, Art. no. 6400206, doi: 10.1109/TASC.2013.2237873.

[18] J. Jiang et al., "Performance and microstructure variation with maximum heat treatment temperature for recent Bi-2212 round wires," *IEEE Trans. Appl. Supercond.*, vol. 33, no. 5, Aug. 2023, Art. no. 6400105, doi: 10.1109/TASC.2023.3236870.

[19] J. Jiang et al., "Effects of wire diameter and filament size on the processing window of Bi-2212 round wire," *IEEE Trans. Appl. Supercond.*, vol. 31, no. 5, Aug. 2021, Art. no. 6400206, doi: 10.1109/TASC.2021.3055475.

[20] M. R. Matras, J. Jiang, D. C. Larbalestier, and E. E. Hellstrom, "Understanding the densification process of Bi $_2$ Sr $_2$ CaCu $_2$ O $_x$ round wires with overpressure processing and its effect on critical current density," *Supercond. Sci. Technol.*, vol. 29, no. 10, Oct. 2016, Art. no. 105005, doi: 10.1088/0953-2048/29/10/105005.

[21] S. I. Hossain, "Understanding the role of wire architecture in determining the critical current performance of Bi-2212 round wire," 2022, Accessed: Sep. 25, 2024. [Online]. Available: https://repository.lib.fsu.edu/islandora/object/fsu%3A826746/

[22] T. A. Oloye et al., "Correlation of critical current density to quasi-biaxial texture and grain boundary cleanliness in fully dense Bi-2212 wires," *Supercond. Sci. Technol.*, vol. 34, no. 3, Mar. 2021, Art. no. 035018, doi: 10.1088/1361-6668/abd575.